GPCR-specific autoantibody signatures are associated with physiological and pathological immune homeostasis.
Cabral-Marques et al.

Supplementary Figure 1

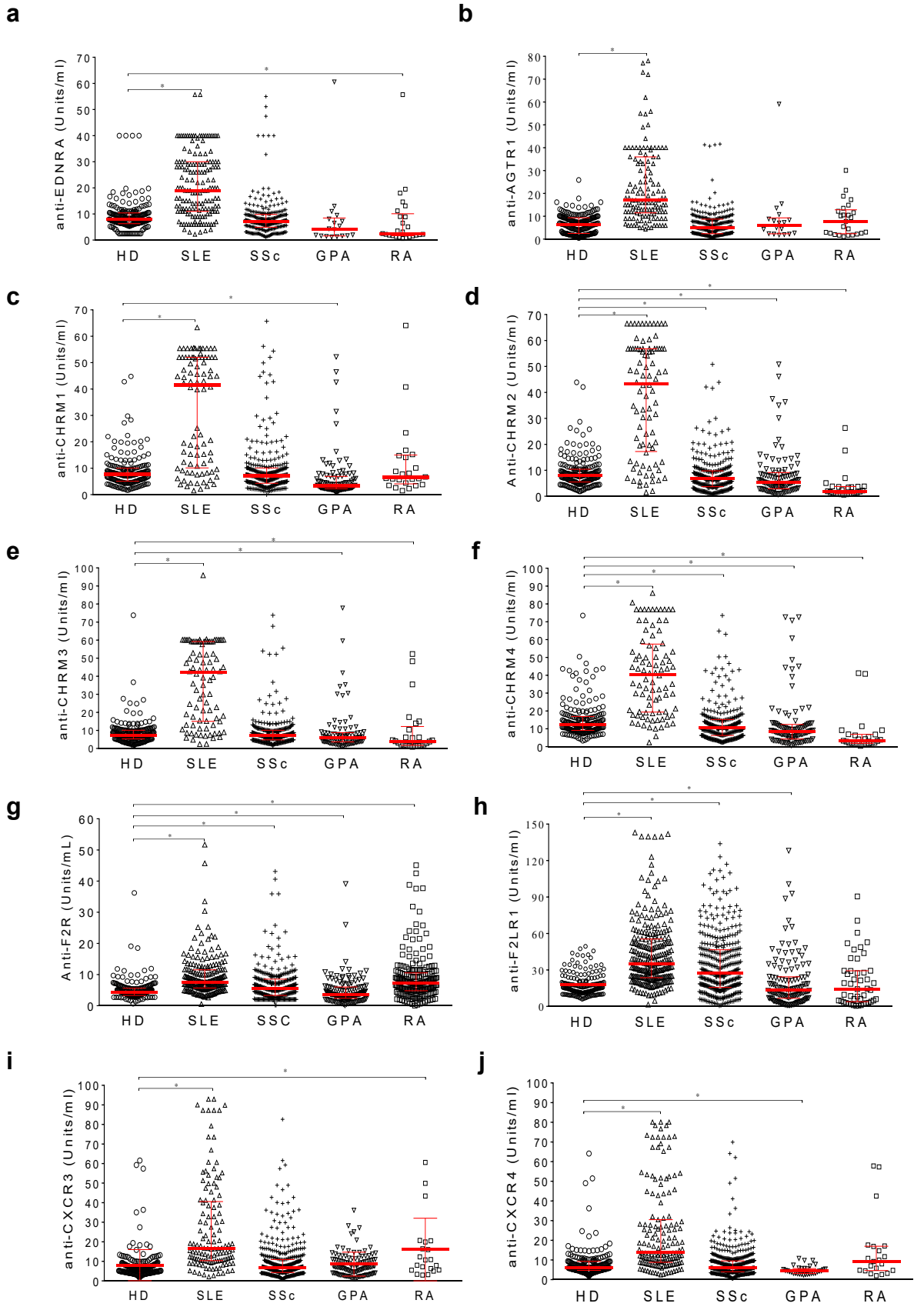

Supplementary Figure 1. Dysregulation of autoantibody concentrations in patients with autoimmune diseases. Graphics show the concentrations of aab directed against A-J) 10 different GPCRs, comparing healthy donors (HD, n=197) to patients with autoimmune diseases. A total of 249 patients with systemic lupus erythematosus (SLE), 379 patients with systemic sclerosis (SSc), 128 patients with granulomatosis with polyangiitis (GPA), and 196 with rheumatoid arthritis (RA) were screened in this phase of the investigation. However, not all patients could be screened for the 10 aab due to sample limitations. The median with interquartile range is shown in red. *, $p<0.05$ (Mann-Whitney test).

Supplementary Figure 2

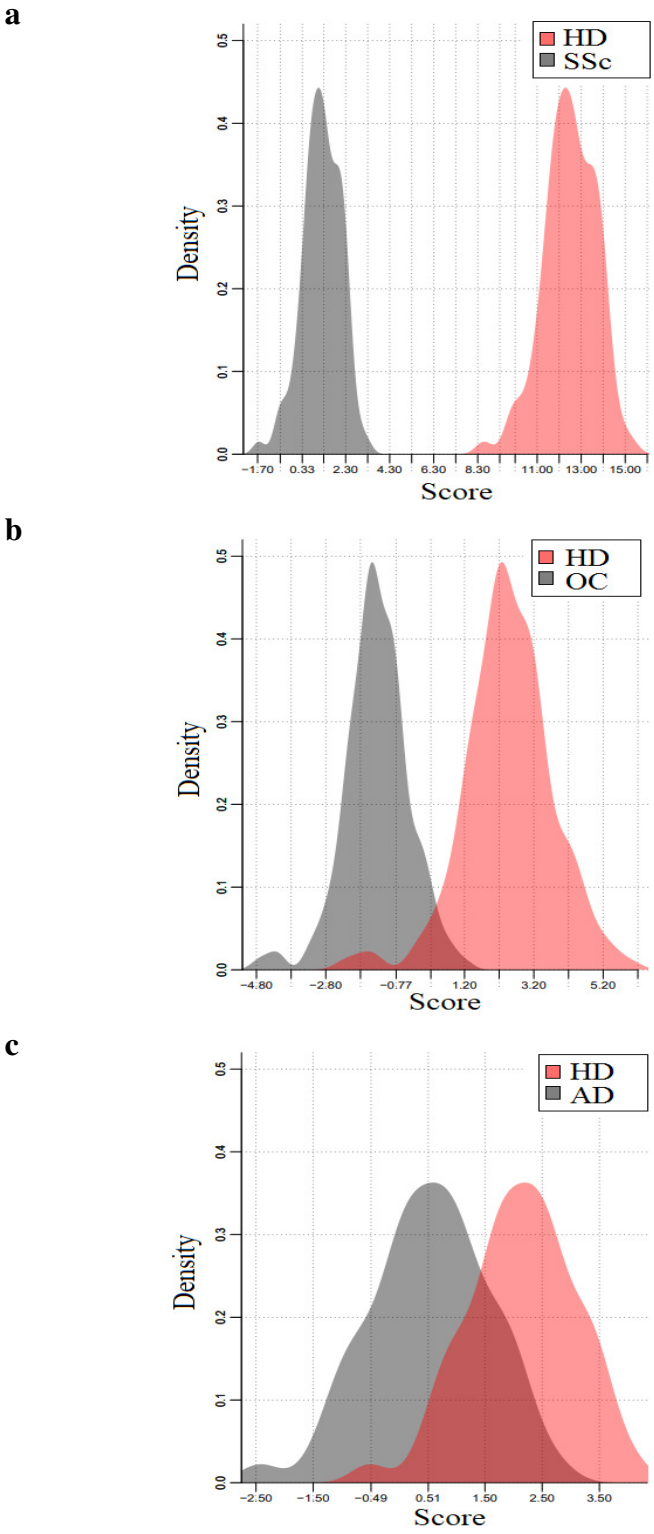

Supplementary Figure 2. Linear discriminant analysis of autoantibody signatures differentiates healthy subjects and patients. Density plots of the linear discriminating scores show the separation between individuals belonging to the disease groups compared with healthy donors (HD). A) HD versus patients with systemic sclerosis (SSc, Supplementary Table 1, cohort 1; Supplementary Table 2, aab dataset 1, B) HD versus patients with ovarian cancer (OC, Supplementary Table 1, cohort 2; Supplementary Table 2, aab dataset 2), and C) HD versus patients with Alzheimer's disease (AD, Supplementary Table 1, cohort 3; Supplementary Table 2, aab dataset 3).

Supplementary Figure 3

a

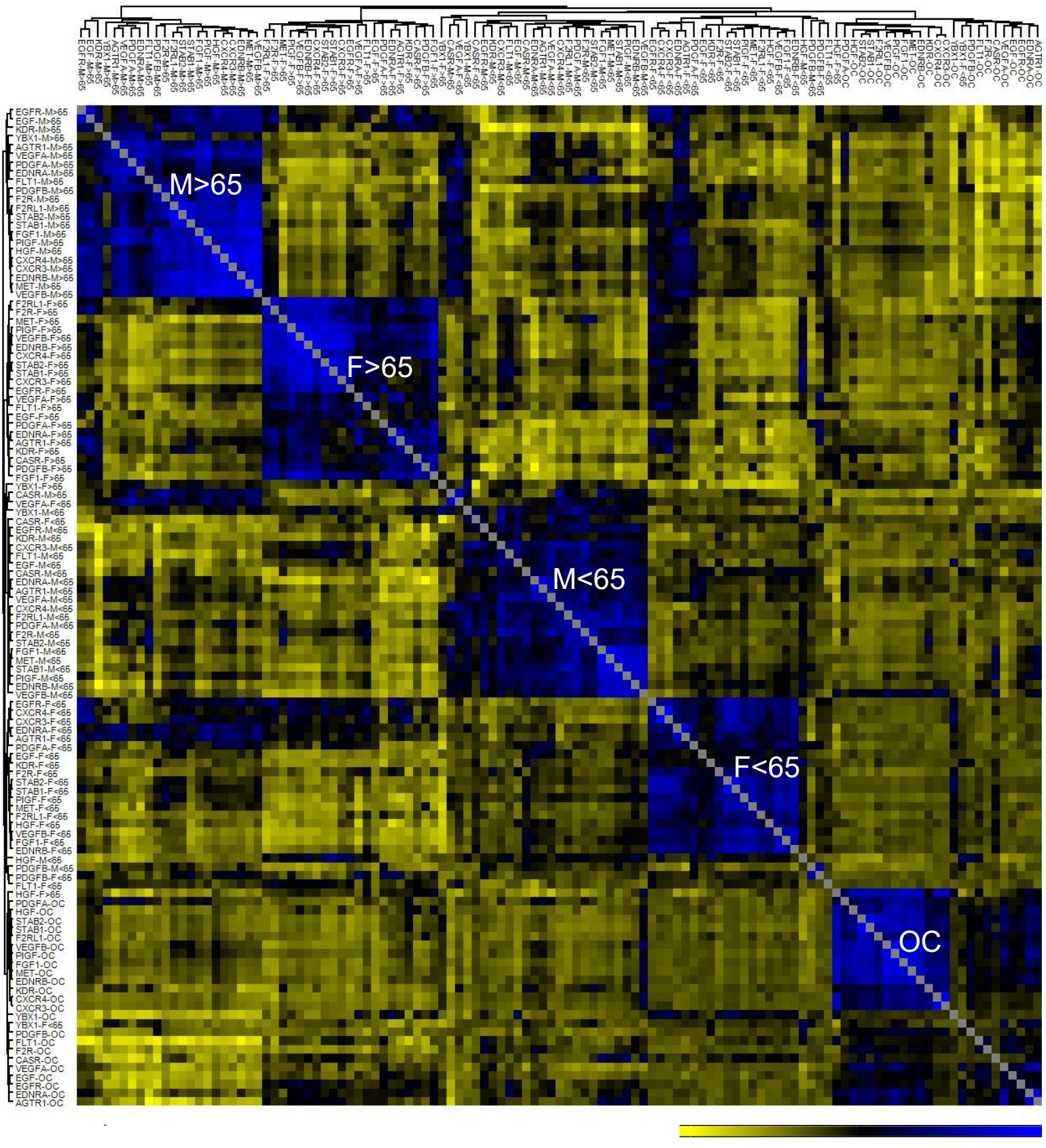

b

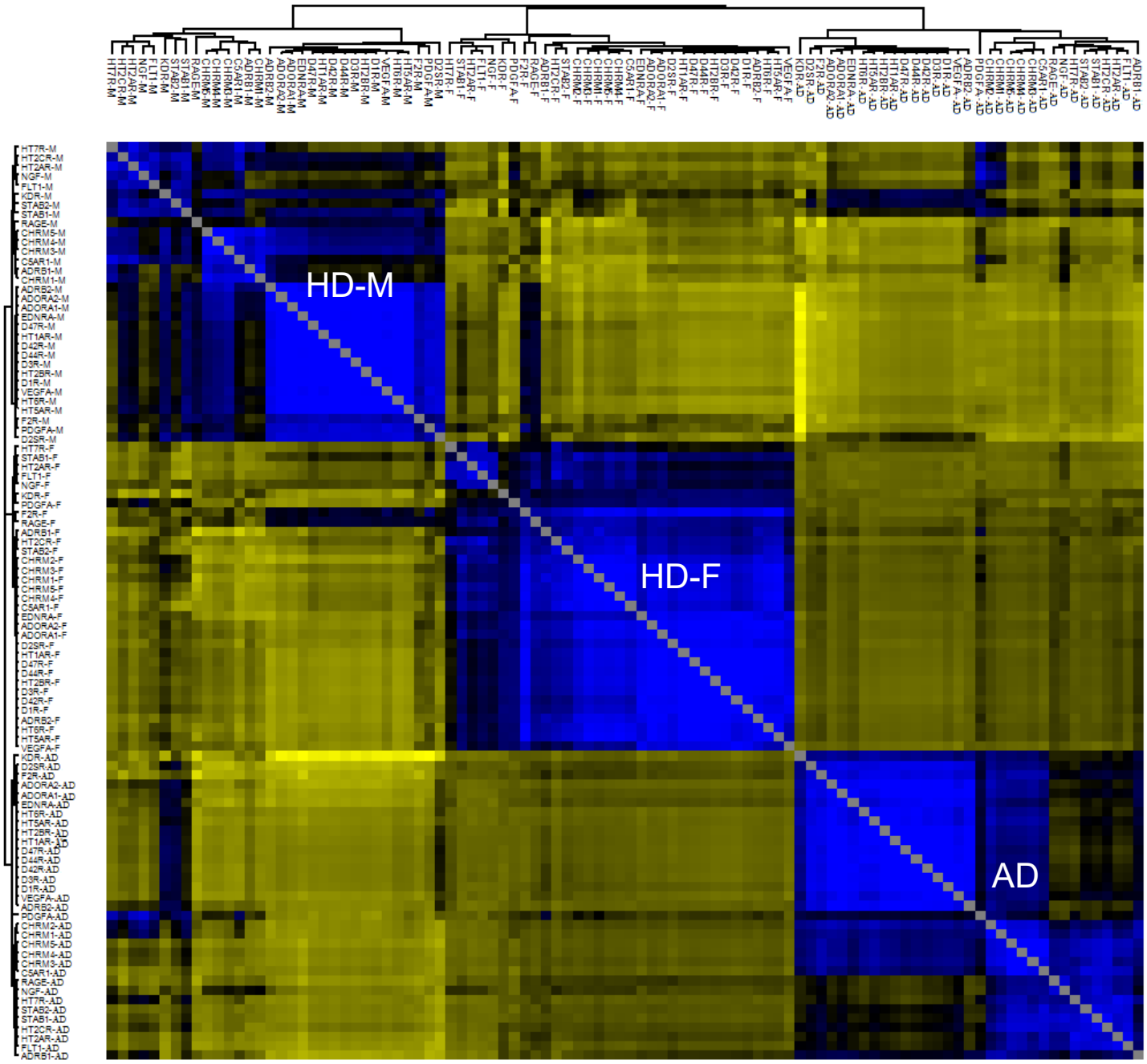

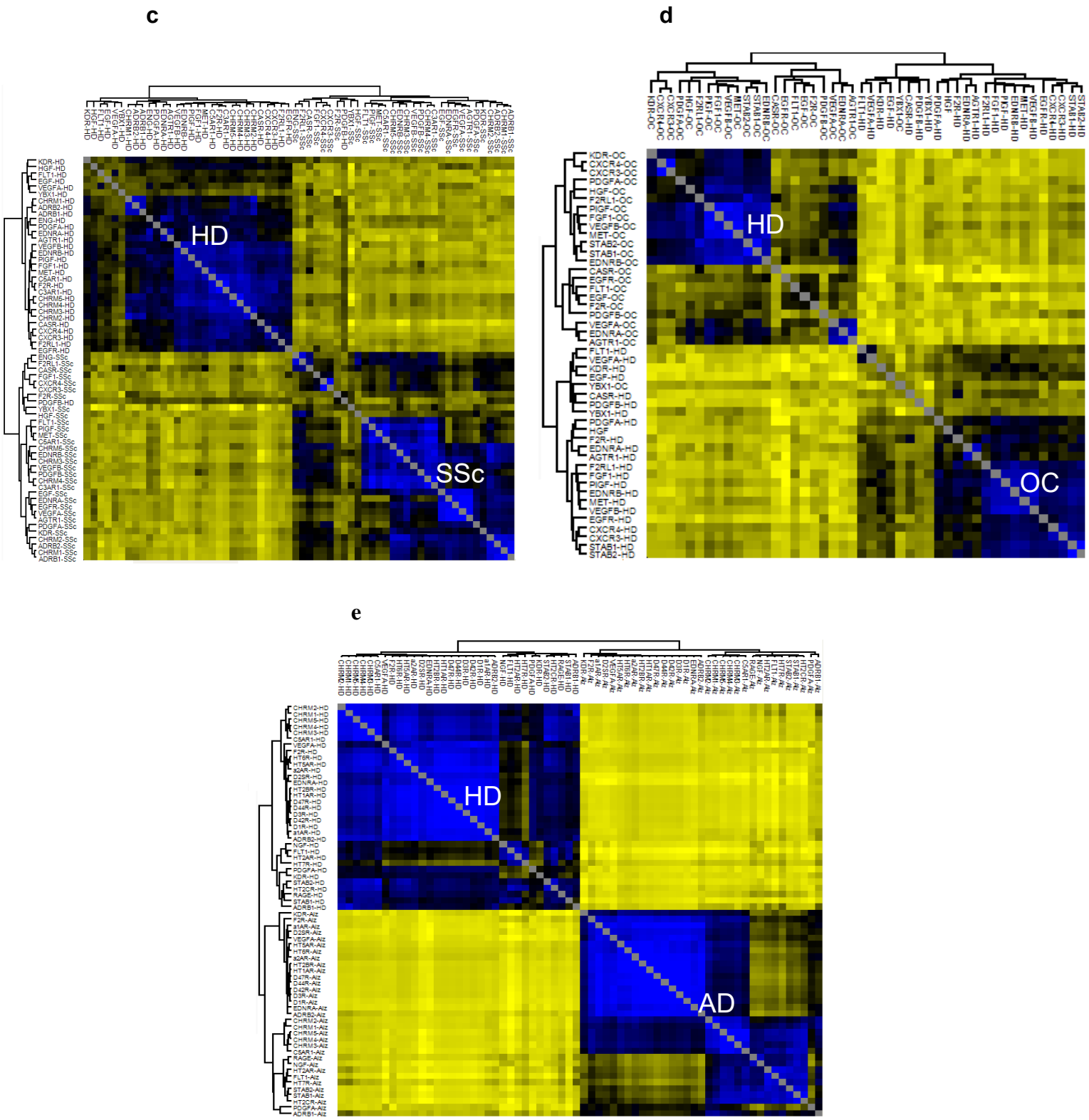

Supplementary Figure 3. Hierarchical clustering analysis reveals autoantibody correlation signatures according to gender, age and diseases. Correlogram matrices display clusters of aab. A) The heatmap displays the clusters of aab correlations from subgroups (females and males aged < and ≥65 years) of healthy donors (HD) versus ovarian cancer (OC; Supplementary Table 1, cohort 2; Supplementary Table 2, aab dataset 2). B) HD in relation to patients with Alzheimer's disease (AD, Supplementary Table 1, cohort 3; Supplementary Table 2, aab dataset 3). The correlation matrices used to perform the hierarchical correlogram of OC and AD are provided as source data. Due to the small number of healthy males <65 years of age (HD cohort 3), we only performed hierarchical clustering analysis of this group according to gender. Supplementary Table 1 provides further details about the HD and patient groups. Analyses of nonsubgrouped C) HD compared with systemic sclerosis (SSc), D) HD versus ovarian cancer (OC), E) and HD in relation to patients with Alzheimer's disease (AD) are shown. Dendrograms on the top and side of the correlation matrix display clusters of correlation between aab. In the heatmap matrix, each small square represents a pairwise correlation between aab. The bar ranging from yellow to blue (A-B: -0.5 to 0.9; C-E: -0.3 to 1) represents negative to positive correlations, respectively.

Supplementary Figure 4

a

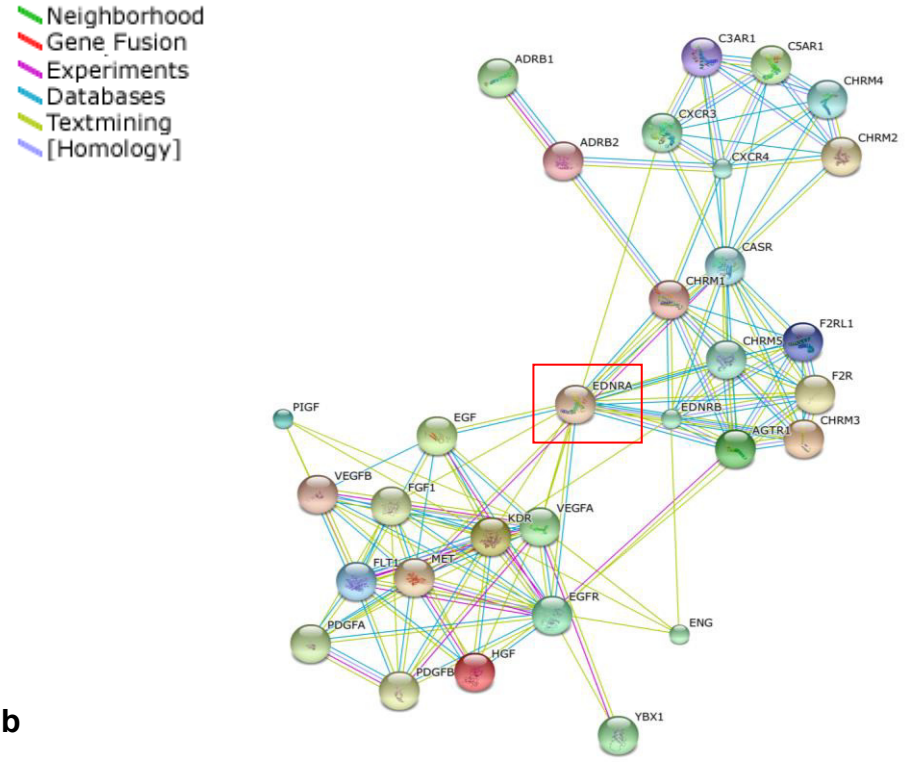

b

GO Term	GO Biological Process	Molecules	p-value_FDR
GO:0030334	regulation of cell migration	VEGFA, HGFR, ENG, VEGFR1, CXCR3, PAR1, VEGFB, CXCR4, C3AR1, HGF, FGF1, EDNRA, VEGFR2, PDGFA, EGFR	1.26^{-12}
GO:0007200	phospholipase C-activating G-protein coupled receptor signaling pathway	M5, EDNRA, CASR, M1, M3, PAR1, M2, M4, AGTR1	1.26^{-12}
GO:0040017	positive regulation of locomotion	VEGFB, HGFR, CASR, VEGFR1, CXCR3, PAR1, C3AR1, HGF, FGF1, EDNRA , VEGFR2, PDGFA, EGFR	1.26^{-12}

Supplementary Figure 4. Network and gene ontology analysis of autoantibody targets. To help interpret the biological meaning of a putative physiological aab network, we performed gene ontology analysis of aab targets (Extended Data Tab 2, aab dataset 1) using the STRING database. A) Differently colored lines represent different forms of relationship evidence: red lines represent the presence of fusion evidence; green lines show neighborhood evidence; blue lines display cooccurrence evidence; purple lines exhibit experimental evidence; yellow lines demonstrate text mining evidence; and light blue lines display database evidence. The red frame indicates EDNRA in the center of the network. B) The lower panel lists physiological functions regulated by interactions between GPCRs and growth factors or related signaling molecules. Enriched gene ontology (GO) biological processes were considered when the false discovery rate (FDR) was less than 0.05.

Supplementary Figure 5

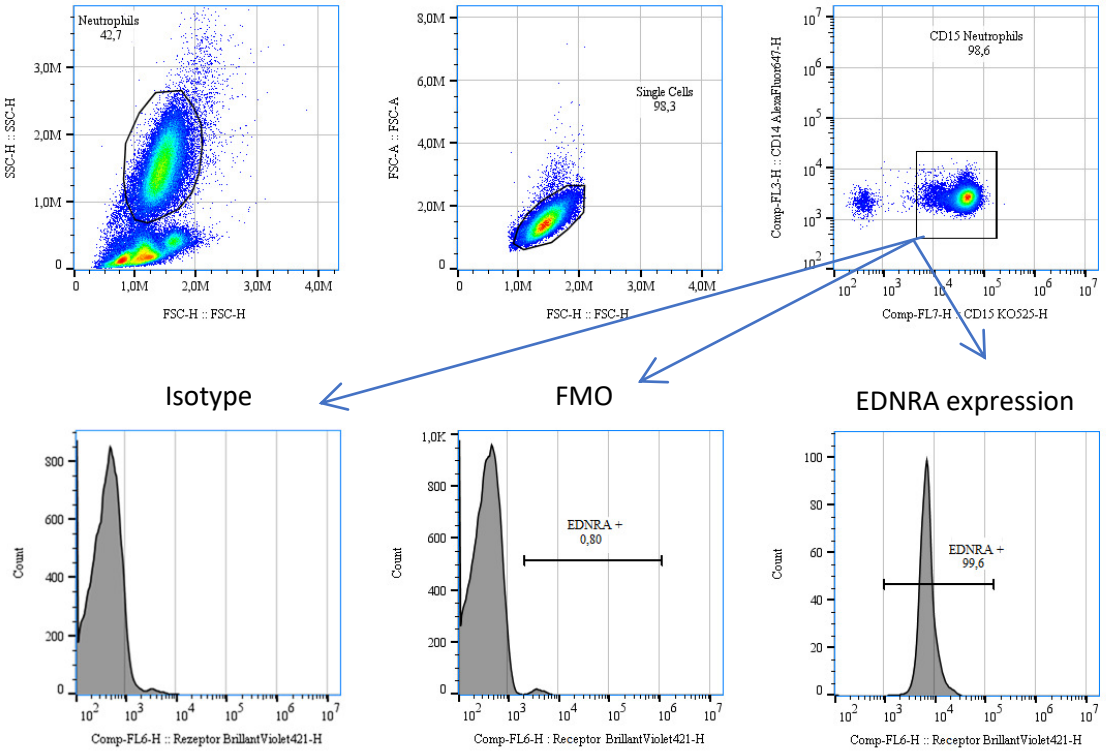

Supplementary Figure 5. Gating strategy for EDNRA expression. For MFI values, an isotype control (Supplementary Table 3) was used to compensate for changes in the cytometry instrument sensitivity. Considering the multiple fluorochromes in the antibody panel to analyze EDNRA expression (Supplementary Table 3), the fluorescence minus one (FMO) control was determined when all the antibodies were present in the flow cytometry tube, except the antibody used to measure EDNRA expression.

Supplementary Figure 6

a

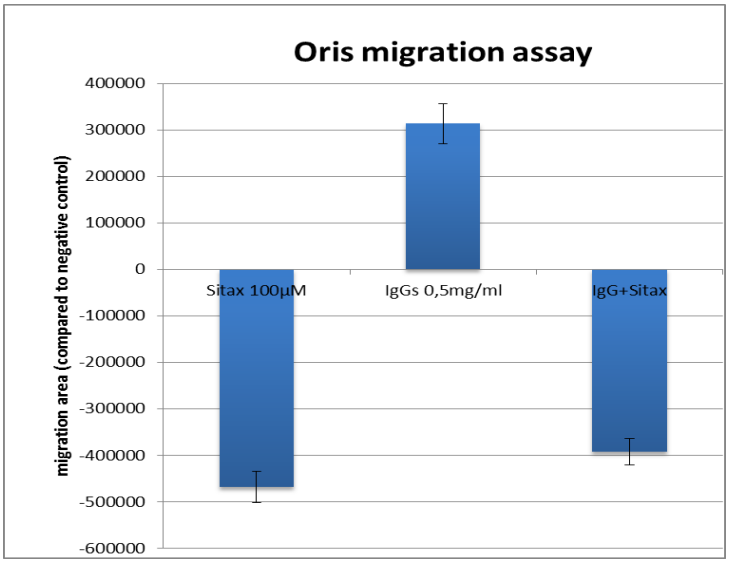

b

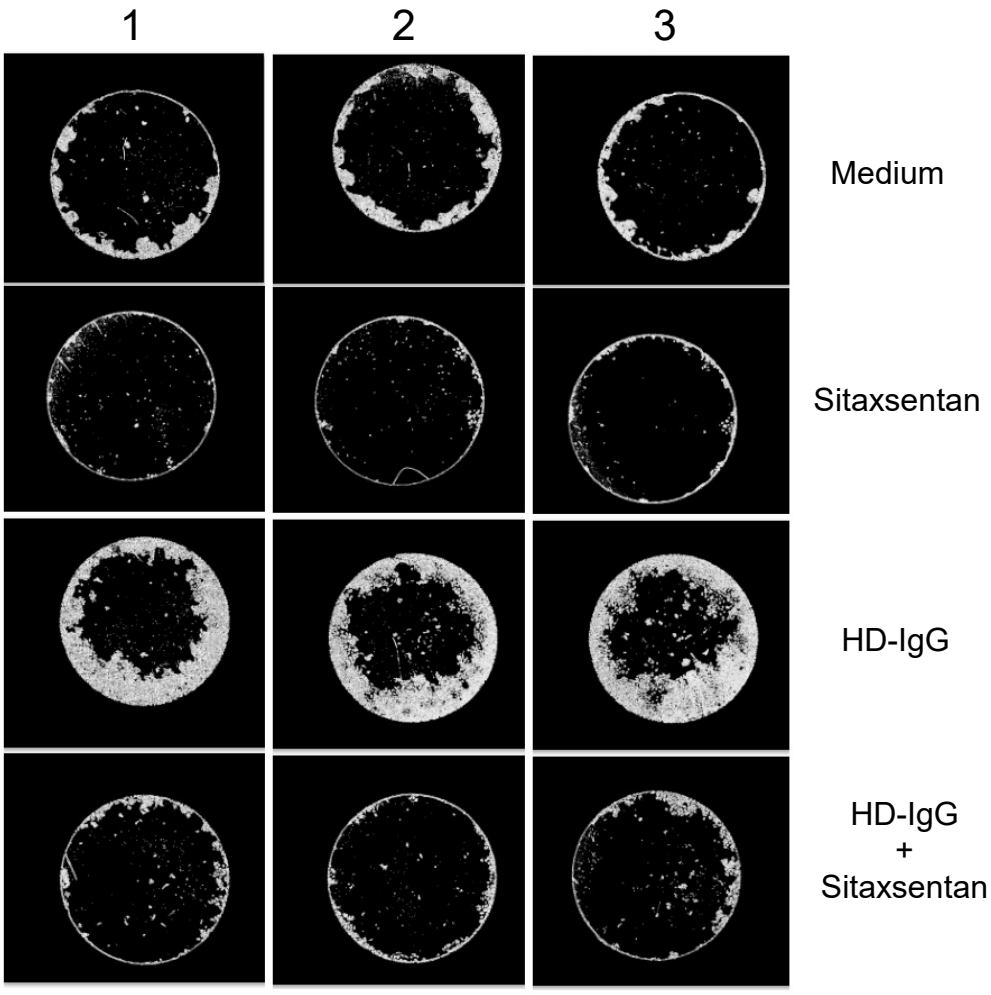

Supplementary Figure 6. Effect of HD-IgG on the migration of the human pancreatic carcinoma Colo357 cell line. The chemotaxis of 3x105 (cells/well) human pancreatic carcinoma Colo357 toward 0.5 mg/ml IgG from healthy donors (HD-IgG) was analyzed using the cell-based Oris™ migration assay. A) The migration area was determined by analyzing B) migration images with the Fiji module of the ImageJ software. Assays were performed in triplicate (1, 2, 3, at the top of the figure). One of three independent experiments (n = 3) is shown. Error bars denote SD. *, $p<0.05$.

Supplementary Figure 7

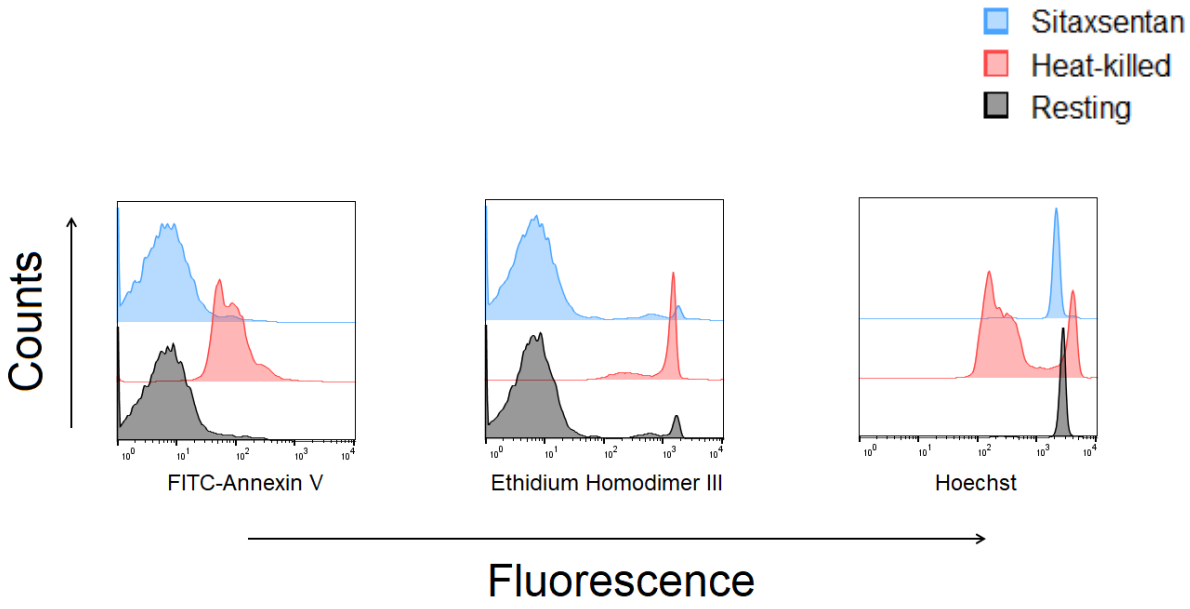

Supplementary Figure 7. Exposure to sitaxsentan, a potent endothelin receptor type A antagonist, has no toxic effect on neutrophils. Neutrophil apoptosis or necrosis was assessed by flow cytometric analysis. The histogram on the left displays apoptotic cells stained by FITC-annexin V; the middle histogram shows necrotic cells stained with ethidium homodimer-III; the histogram on the right demonstrates healthy donor cells stained with Hoechst. Heat-killed cells were used as the experimental control. The results are representative of three independent experiments. The effects of sitaxsentan on neutrophil survival were analyzed by flow cytometry using the Apoptotic/Necrotic/ Healthy Cells Detection Kit (PromoCell, Heidelberg, Germany) according to the manufacturer's instructions.

Supplementary Figure 8

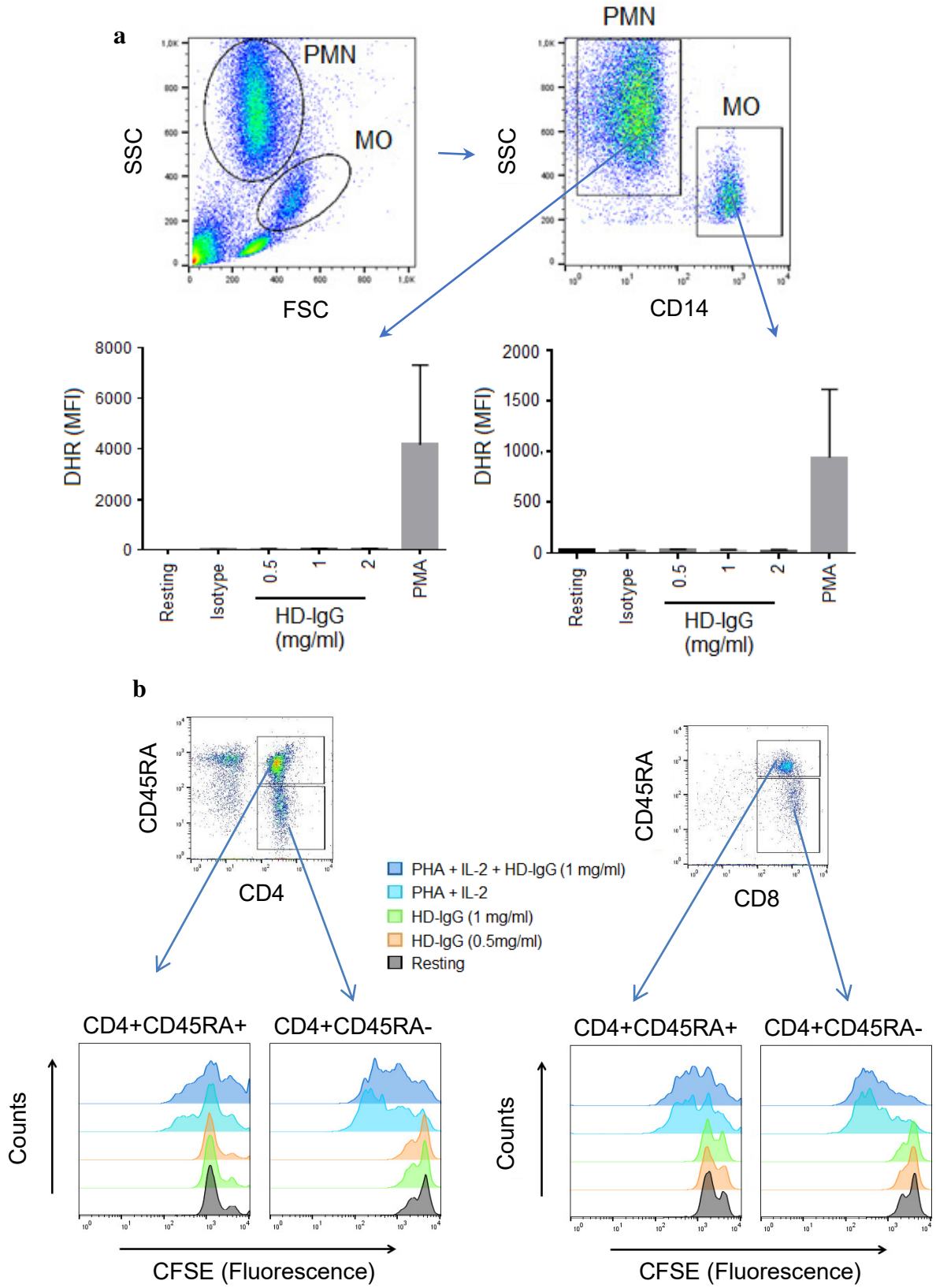

Supplementary Figure 8. Normal human IgG has no effect on the respiratory burst of phagocytes and T cell proliferation. A) The 300 ng/ml phorbol-12-myristate-13-acetate (PMA) but not 0.5 mg/ml healthy donor (HD) IgG induces the respiratory burst of polymorphonuclear neutrophils (PMN) and monocytes (MO). White blood cells were stimulated in vitro in the presence of PMA for 60 min and analyzed by flow cytometry following 400 ng/ml dihydrorhodamine (DHR) 123 staining. Neutrophils and monocytes were gated according to size (forward scatter, FSC), granularity (side scatter, SSC) and pattern of CD14 expression. The median fluorescence intensity (MFI) of the respiratory burst from three different experiments is shown. Error bars denote SD. (B) PBMCs were isolated by Ficoll-Paque density gradient sedimentation. After 5 days at 37°C in the absence or presence of 5 µg/ml phytohemagglutinin (PHA)/10 U/ml of IL-2, robust cell proliferation was observed, but no effect was observed with HD-IgG (n = 3).

Supplementary Figure 9

a

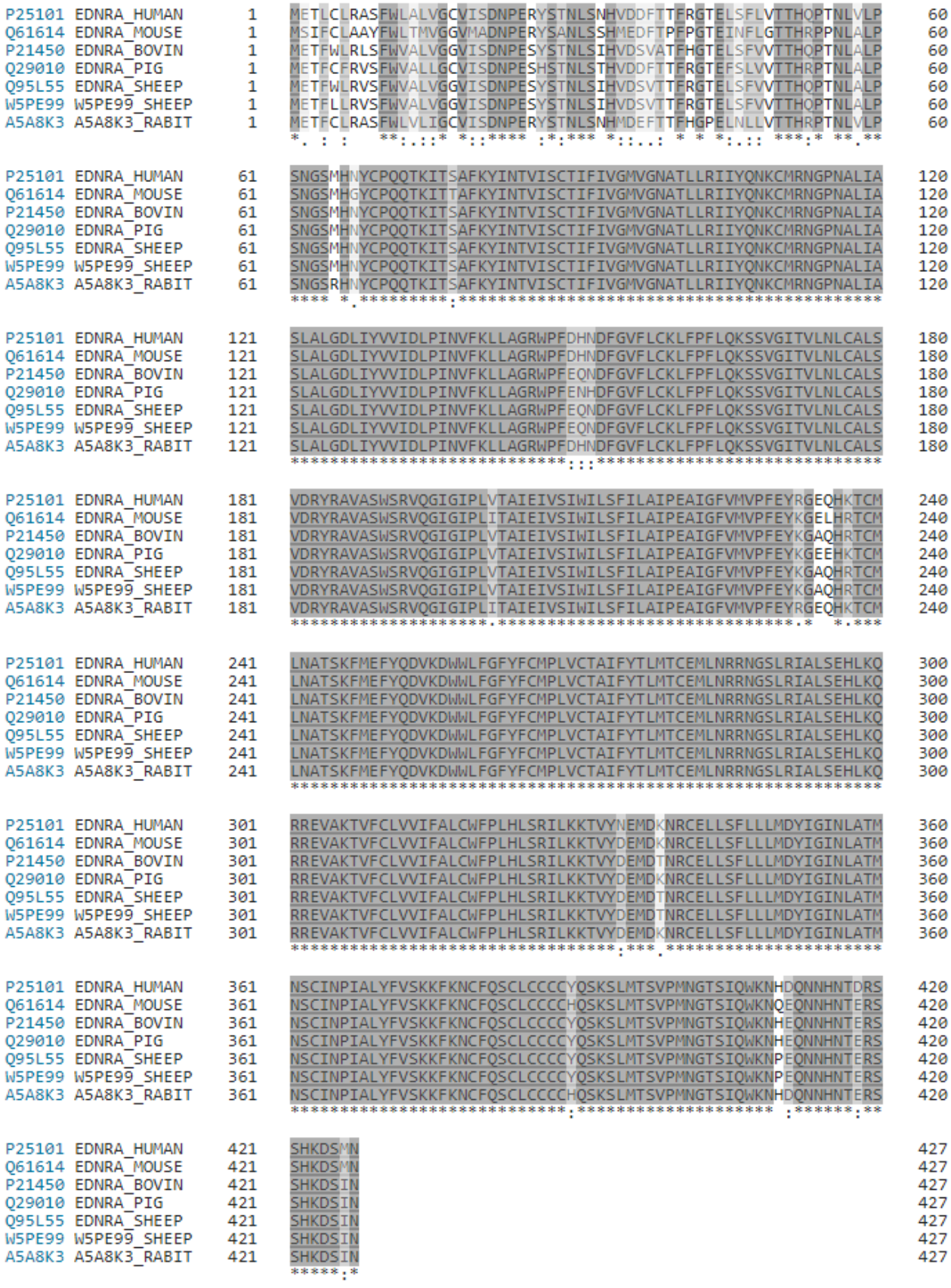

b

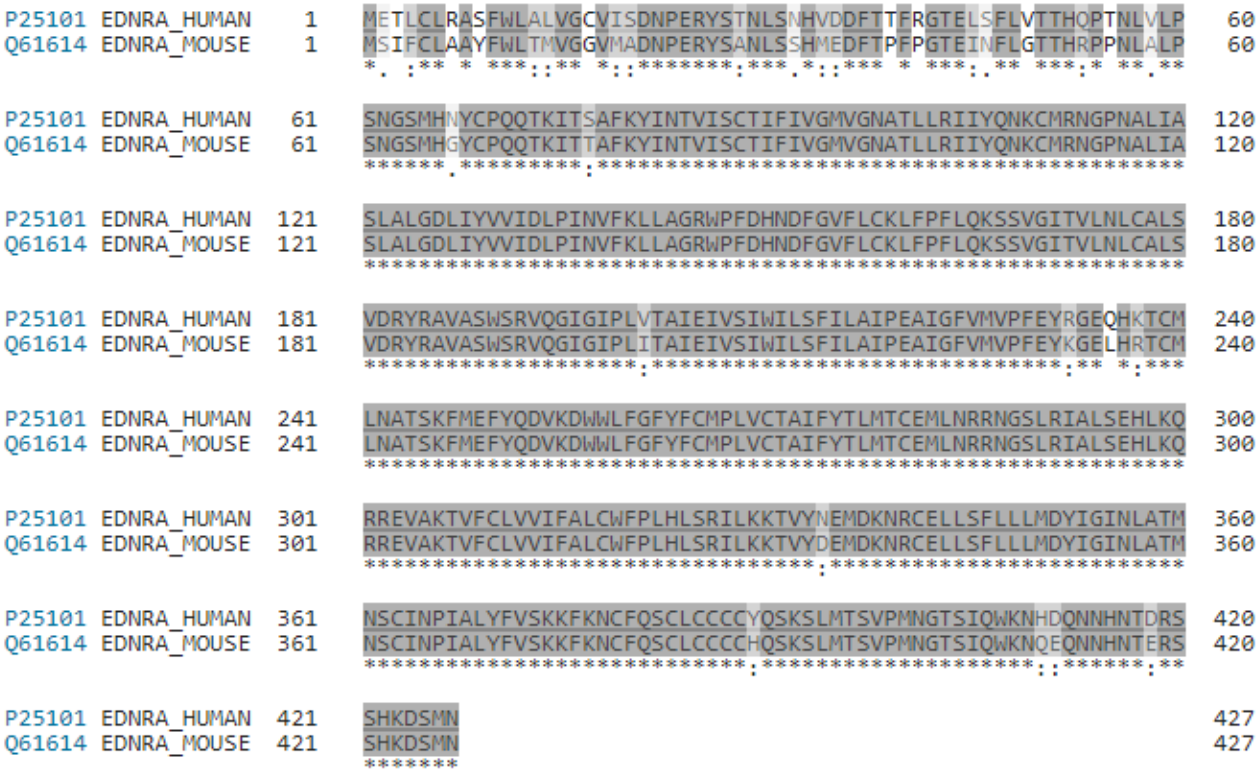

Supplementary Figure 9. Sequence alignment of endothelin receptor type A. A) A multiple sequence alignment of endothelin receptor type A (EDNRA) shows the high conservation (87.58% identical) among different species and between B) Homo sapiens and Mus musculus (92.27% identical). Alignment of EDNRA was performed using the Clustal Omega program (https://www.UniProt.org/align/) and EDNRA UniProt identifiers.

Supplementary Table 1

HD (cohort 1	*<65*	*≥65*	*total*	*Mean Age*
male	42	24	66	60.3 ± 7.8
female	104	23	127	57.6 ± 7.2
total	146	47	193	58.5 ± 7.5
Systemic Sclerosis	*<65*	*≥65*	*total*	*Mean Age*
male	1	13	14	52.8 ± 9.4
female	62	8	70	56.9 ± 13
total	63	21	84	56.2 ± 12.5

HD (cohort 2	*<65*	*≥65*	*total*	*Mean Age*
male	43	23	66	60.4 ± 7.9
female	104	25	129	57.7 ± 7.1
total	147	48	195	58.9 ± 7.5
Ovarian cancer	*<65*	*≥65*	*total*	*Mean Age*
male	0	0	0	0
female	141	66	207	59.1 ± 11.4
total	141	66	207	59.1 ± 11.4

HD (cohort 3	*<65*	*≥65*	*total*	*Mean Age*
male	1	26	27	73.9 ± 6.5
female	11	65	76	72.5 ± 8.6
total	12	91	103	73.5 ± 7.5
Alzheimer´s disease	*<65*	*≥65*	*total*	*Mean Age*
male	4	21	25	73.4 ± 7.9
female	5	61	66	75.8 ± 7.4
total	9	82	91	74.9 ± 7.8

Supplementary Table 1. Demographics of healthy donors and patients. All healthy donors (HD) were German subjects not receiving medications known to have any effect on the immune response. Three different HD cohorts, cohort 1 (upper panel), cohort 2 (middle panel) and cohort 3 (lower panel), were used throughout the study for comparison with patients affected by systemic sclerosis (SSc), ovarian cancer (OC) and Alzheimer's disease (AD), respectively.

Supplementary Table 2

Aab dataset 1 – HD cohort 1 and SSc	Full Name
G protein-coupled receptors	
AT1R or *AGTR1*	angiotensin II receptor type 1
ADRB1	beta-1 adrenergic receptor
ADRB2	beta-2 adrenergic receptor
CASR	calcium-sensing receptor
CXCR3	chemokine (C-X-C motif receptor 3
CXCR4	chemokine (C-X-C motif receptor 4
C3AR1	complement component 3a receptor 1
C5AR1	complement component 5a receptor 1
ETAR or *EDNRA*	endothelin receptor type A
ETBR *EDNRB*	endothelin receptor type B
M1 or *CHRM1*	cholinergic receptor muscarinic 1
M2 or *CHRM2*	cholinergic receptor muscarinic 2
M3 or *CHRM3*	cholinergic receptor muscarinic 3
M4 or *CHRM4*	cholinergic receptor muscarinic 4
M5 or *CHRM5*	cholinergic receptor muscarinic 5
PAR1 or *F2R*	Protease-activated receptor 1
PAR2 or *F2RL1*	Protease-activated receptor 2
Growth factors	
EGF	epidermal growth factor
FGF1	fibroblast growth factor 1
HGF	hepatocyte growth factor
PDGFA	platelet-derived growth factor alpha
PDGFB	platelet-derived growth factor beta
VEGFA	vascular endothelial growth factor A
VEGFB	vascular endothelial growth factor B
PIGF	Placental growth factor
Growth factor receptors	
EGFR	epidermal growth factor receptor
HGFR or *MET*	hepatocyte growth factor receptor
VEGFR1 or *FLT1*	vascular endothelial growth factor 1
VEGFR2 or *KDR*	vascular endothelial growth factor 2
Signaling molecules	
YBX1	Y-box-binding protein 1
ENG	Endoglin

Aab dataset 2 - HD cohort 2 and OC	Full Name
G protein-coupled receptors	
AT1R or *AGTR1*	angiotensin II receptor type 1
CASR	calcium-sensing receptor
CXCR3	chemokine (C-X-C motif receptor 3
CXCR4	chemokine (C-X-C motif receptor 4
ETAR or *EDNRA*	endothelin receptor type A
ETBR *EDNRB*	endothelin receptor type B
PAR1 or *F2R*	Protease-activated receptor 1
PAR2 or *F2RL1*	Protease-activated receptor 2
Growth factor receptors	
EGF	epidermal growth factor
FGF1	fibroblast growth factor
HGF	hepatocyte growth factor
PDGFA	platelet-derived growth factor alpha
PDGFB	platelet-derived growth factor beta
VEGFA	vascular endothelial growth factor A
VEGFB	vascular endothelial growth factor B
PIGF	Placental growth factor
Growth factor receptors	
EGFR	epidermal growth factor receptor
HGFR or *MET*	hepatocyte growth factor receptor
VEGFR1 or *FLT1*	vascular endothelial growth factor 1
VEGFR2 or *KDR*	vascular endothelial growth factor 2
Signaling molecules	
YBX1	Y-box-binding protein 1
Scavenger receptors	
STAB1	Stabilin-1
STAB2	Stabilin-2

Aab dataset 3 – HD cohort 3 and AD	Full Name
G protein-coupled receptors	
ADRB1	beta-1 adrenergic receptor
ADRB2	beta-2 adrenergic receptor
C5AR1	complement component 5a receptor 1
ETAR or *EDNRA*	endothelin receptor type A
M1 or *CHRM1*	cholinergic receptor muscarinic 1
M2 or *CHRM2*	cholinergic receptor muscarinic 2
M3 or *CHRM3*	cholinergic receptor muscarinic 3
M4 or *CHRM4*	cholinergic receptor muscarinic 4
M5 or *CHRM5*	cholinergic receptor muscarinic 5
PAR1 or *F2R*	Protease-activated receptor 1
Growth factors	
PDGFA	platelet-derived growth factor alpha polypeptide
VEGFA	vascular endothelial growth factor A
Growth factor receptors	
VEGFR1 or *FLT1*	vascular endothelial growth factor 1
VEGFR2 or *KDR*	vascular endothelial growth factor 2
Neurological or AD-associated Molecules	
α_1AR	Alpha 1 adrenoceptor
α2AR	Alpha 2 adrenoceptor
D1R	D1 Dopamine receptor
D2SR	D2s Dopamine receptor
D3R	D3 Dopamine receptor
D42R	D42 Dopamine receptor
D44R	D44 Dopamine receptor
D47R	D47 Dopamine receptor
HT1AR	5-hydroxytryptamine receptor 1
HT2AR	5-hydroxytryptamine receptor 2A
HT2BR	5-hydroxytryptamine receptor 2B
HT2CR	5-hydroxytryptamine receptor 2C
HT5AR	5-hydroxytryptamine receptor 5
HT6R	5-hydroxytryptamine receptor 6
HT7R	5-hydroxytryptamine receptor 7
NGF	Nerve growth factor beta
RAGE	Receptor for advanced glycation end products
Signaling molecules	
YBX1	Y-box-binding protein 1
ENG	Endoglin
Scavenger receptors	
STAB1	Stabilin-1
STAB2	Stabilin-2

Supplementary Table 2. Autoantibody datasets. Three datasets of autoantibodies (aab) were analyzed in sera from three healthy donor (HD) cohorts and patients with systemic sclerosis (SSc, upper left panel), ovarian cancer (OC, lower left panel) and Alzheimer's disease (AD, upper right panel).

Supplementary Table 3

Antibodies				
Antibody targets	*Fluorochrome*	*Dilution*	*Clone or number*	*Manufacturer*
CD14	PE-Cy7/Alexa Fluor 647	1:200/1:50	HCD14/ M5E2	Biolegend
CD15	Brillant Violet 510	1:50	W6D3	Biolegend
Anti-Rabbit IgG	CFL405	1:100	Sc-362252	SantaCruz
Anti-Rabbit IgG	Brillant Violet 421	1:500	Poly4064	Biolegend
EDNRA	n.a.	1:100	sc-33535	Santa Cruz
Isotype 1	n.a.	1:100	sc-3888	Santa Cruz

Supplementary Table 3. Antibody panel used for flow cytometric analyses of EDNRA expression.